Optics and Lasers in Engineering 106 (2018) 61–67

Contents lists available at ScienceDirect

Optics and Lasers in Engineering

journal homepage: www.elsevier.com/locate/optlaseng

Localized analysis of paint-coat drying using dynamic speckle interferometry

Daniel Sierra-Sosa[a,*], Myrian Tebaldi[b], Eduardo Grumel[b], Hector Rabal[b], Adel Elmaghraby[a]

[a] Department of Computer Engineering and Computer Science, Duthie Center for Engineering, University of Louisville, Louisville, KY 40292, USA
[b] Centro de Investigaciones Ópticas (CONICET La Plata-CIC-UNLP) and UIDET OPTIMO, Departamento de Ciencias Básicas, Facultad de Ingeniería, Universidad Nacional de La Plata, P.O. Box 3 C.P 1897, La Plata, Argentina

ARTICLE INFO

Keywords:
Dynamic speckle
Paint-coating drying
Co-occurrence matrix

ABSTRACT

The paint-coating is part of several industrial processes, including the automotive industry, architectural coatings, machinery and appliances. These paint-coatings must comply with high quality standards, for this reason evaluation techniques from paint-coatings are in constant development. One important factor from the paint-coating process is the drying, as it has influence on the quality of final results. In this work we present an assessment technique based on the optical dynamic speckle interferometry, this technique allows for the temporal activity evaluation of the paint-coating drying process, providing localized information from drying. This localized information is relevant in order to address the drying homogeneity, optimal drying, and quality control. The technique relies in the definition of a new temporal history of the speckle patterns to obtain the local activity; this information is then clustered to provide a convenient indicative of different drying process stages. The experimental results presented were validated using the gravimetric drying curves

1. Introduction

When an optically rough surface is illuminated by coherent light, a granular high contrast pattern distributed in space with a homogeneous mean intensity can be observed–these patterns are known as speckle. Characteristics of speckle are related to the macroscopic properties of the illuminated surface under analysis [1].

Over the years several speckle measurement techniques have being developed. Some of those techniques rely in the changes over time of the speckle patterns. The dynamic speckle phenomenon occurs when laser light is scattered by samples with a time-dependent activity, for example to characterize fruit slices, confirm seed viability, fungi detection and ultrasound imaging [2–7].

The activity could be observed in non-biological and biological samples and it is a consequence of the changes in the phase of light produced, for example, by movements of the scatters centers. As analyzed in several contributions, the mentioned effect produces variation in local intensity known as “boiling speckle” due to its visual appearance.

In a previous work, dynamic speckle pattern method was applied to study the drying of paint process [8-10]. The dynamic speckle pattern is generated when the paint surface is illuminated with coherent light. In fact, the illuminated surface changes mainly due to solvent evaporation and layer formation, thus giving rise to mentioned speckle activity. Amalvy et al. [8] introduced the use of the co-occurrence matrix of the time history from dynamic speckle pattern as a method to measure the activity. The temporal history of the speckle pattern (THSP) is generated by setting side by side a certain column of pixels corresponding to successive images. The activity of the THSP image appears as intensity changes in the horizontal direction.

Different descriptors to address the dynamic speckle patterns activity using THSP have been developed, including some based on wavelets transforms [10-12], taking as a starting point, the sequence of data generated in the original work of Amalvy et al. In particular, the authors demonstrate that all the measures tested performs better than the one used in the original work. It should be noted that with these methods provide a global assessment of the paint drying process and could not be used to determine the local evolution.

In [8] the image is divided into columns and the middle one is used in each speckle image in order to generate the THSP. The column is purposely selected in the center of the speckle pattern record. This supposition considers small activity changes along the center of the sample as compared to the edges. However, the activity change is related to the paint layer thickness.

Therefore, we propose an alternative method in order to identify areas with different activity in the drying of paints process. This dynamic speckle method can be used to evaluate the local activity on the surface, by means of a new temporal view of intensity levels The speckle images

* Corresponding author.
E-mail address: d.sierrasosa@louisville.edu (D. Sierra-Sosa).

https://doi.org/10.1016/j.optlaseng.2018.02.013
Received 5 December 2017; Received in revised form 16 February 2018; Accepted 18 February 2018

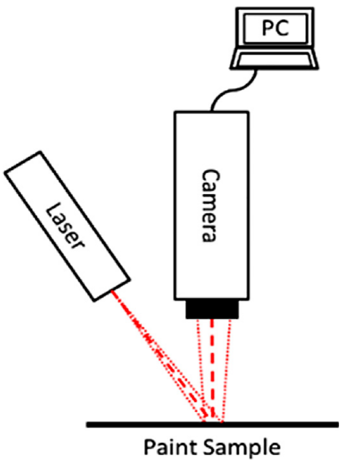

Fig. 1. Experimental setup schema for dynamic speckle recording and coating thickness in samples.

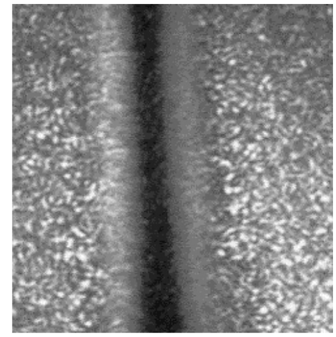

Fig. 2. Recorded speckle samples for local drying evaluation.

are subdivided in 5 × 5 pixels sub-images. Then, a 2-dimensional temporal history speckle pattern (2D-THSP) can be obtained by adequate gathering and processing successive speckle images. As in the conventional case, the 2D-THSP image shows a temporal variation of the gray levels of each pixel of the original speckle along the horizontal axis, nonetheless, the local activity can be evaluated.

The drying process of latex paint is accompanied to the loss of weight as it dries [8]. We also performed a gravimetric measurement in order to validate the proposed method and the experimental results obtained were compared with the gravimetric technique. We found that the resulting curves from the speckle-time evolution compares favorably with gravimetric drying curves.

2. Dynamic speckle: experimental arrangement

On the scale of an optical wavelength ($\lambda \approx 700$ nm) the paint surfaces are rough. It means that when coherent light coming from a laser is scattered by these surfaces speckle patterns appear as the sum of multiple independent complex components with random amplitude, random phase or both.

During the drying process, the coating's surface is changing mainly due to the solvent evaporation, leveling and particle diffusion. Then, the light scattered by paint surface presents a time-dependent activity. The associated speckle patterns will change over time as the surface changes, leading to the dynamic speckle phenomenon [8].

An experiment was conducted to evaluate the paint-coating drying process using dynamic speckle patterns. These patterns were recorded on different drying stages of a latex painting layer extended over a glass surface. For recording the speckle patterns the experimental set-up depicted in Fig. 1 was used.

An expanded 10 mW Helium–Neon laser beam (with a wavelength $\lambda = 632.8$ nm) attenuated with a neutral density filter illuminates the samples to be analyzed. The paint samples were prepared on a glass substrate using a standard stainless steel drawdown applicator onto a flat substrate. The paint layers were applied horizontally with different wet film thicknesses.

The scattered light is then recorded in a sequence of images, allowing tracking the changes over time thus providing a convenient tool to address the slight changes in the surface related with the drying process. When a phenomenon has low activity, there are less time variations in the speckle patterns. In the limit, when there is no activity at all, the speckle pattern shows no variation in the time direction.

The co-occurrence matrix was then calculated to characterize the speckle pattern activity.

Two paint samples were evaluated simultaneously, one with 50 µm and the other 150 µm thicknesses. In this case, the speckle images generated by both paint surfaces were registered by a EO-10012C CMOS Color USB camera connected to a PC. 8 bits' gray scale images (1000 × 1000 pixels) were recorded in the memory of the computer. An example of these patterns is depicted in Fig. 2, where the left side corresponds to the speckle recorded for 50 µm thickness sample and on the right side the speckle corresponding to the 150 µm sample. Care was taken so that the speckles were well resolved by the camera sensor. After drying approximately for 240 min steady state of the dynamic speckle pattern was reached for both thicknesses, indicating that the paint-coating was dry. 1000 successive images were recorded every 15 min. In our case, we define a frame as the results obtained from processing a set of 1000 images recorded over a period of 15 min in 0.9 s time intervals.

In our experiments, we obtained local measurements from the drying process over regions of interest. All the measurements were made in a motionless air and constant temperature room to limit the variables that affect the drying process. The humidity and temperature were those typical of a laboratory and commonly found during drying processes. The room temperature ranged from 20 °C to 25 °C and the relative humidity ranged from 50% to 70%.

Our proposal was validated by comparing the optical measurements with the conventional gravimetric measurements described by Amalvy et al. in [8]. In this case, a single coating layer with an average thickness of 50 µm was applied over the glass substrate. The glass substrate was located on an analytical scale to measure the weight loss due to the drying process and a sequence of 8-bits gray scale images (512 × 512 pixels) dynamic speckle patterns were registered using a PULNIX TM-6CN CCD monochrome camera connected to a PC.

3. Window Operation: local activity evaluation

From the recorded speckle patterns a region of interest was selected for each of different layers. Two paint coating thickness were used in the experiment, and two regions both of 600 rows × 100 columns where selected on each case. Fig. 3 depicts the selected regions used in the experiment, the region marked with blue is the speckle corresponding to the 50 µm layer and the region marked with red the speckle corresponding with the 150 µm layer.

Each region of interest was cropped in 5 × 5 window matrices; these matrices contain a portion of the speckle pattern, the size of these matrices was selected to represent less than 0.05% of the total image, and could be modified based on the recordings resolution and sampling. Note that the window matrix dimension is selected taking into account a compromise between spatial resolution and statistical behavior. As consecutive recordings were made during the drying process, it is expected that this patterns change over time due to the surface activity related to the coating drying. The 5 × 5 matrices will be considered as windows from the speckle pattern allowing for characterize the activity on each region. These windows do not overlap with each other and cover the

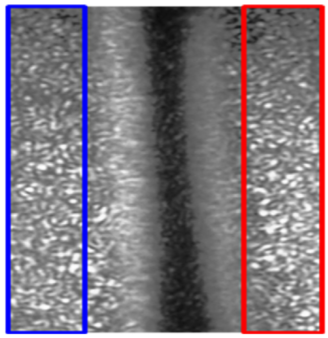

Fig. 3. Recorded speckle patters for experiment and validation, the regions of interest are marked on blue for the 50 µm layer and on red for the 150 µm layer. (For interpretation of the references to color in this figure legend, the reader is referred to the web version of this article).

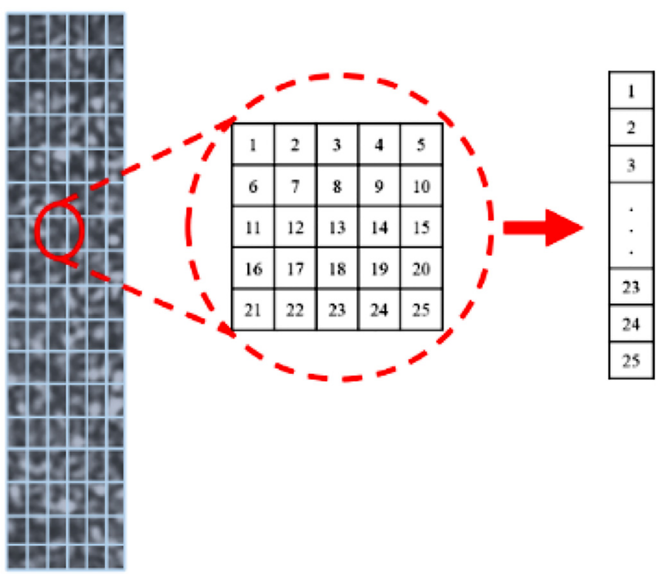

Fig. 4. Windowing operation. The speckle pattern is cropped in 5 × 5 matrices, which are then reshaped as vectors.

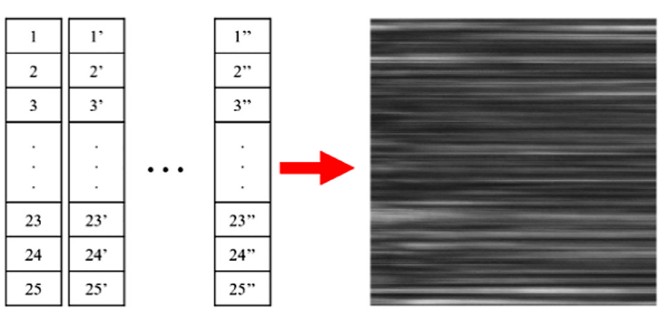

Fig. 5. Window vectors appended and the corresponding temporal history speckle pattern example.

entire region of interest. Each window was then reshaped to obtain a vector with the gray-level values of the speckle pattern as portrayed in Fig. 4, where each row of the 5 × 5 matrix is transposed and appended to form the vector of 25 elements.

From all the vectors obtained for a frame (1000 for the presented experiment), a new 2-dimensional temporal history speckle pattern (2D-THSP) can be obtained per window.

The 2D-THPS is created when the obtained vectors are appended and an image is formed as depicted in Fig. 5. As each position in the vector represents the same point in the window, changes in the horizontal axis represent temporal intensity changes in that particular pixel, the rows in the 2D-THSP are the different pixels in the window and the columns their activity. The original image can be then reconstructed based on the 2D-THSP from each region.

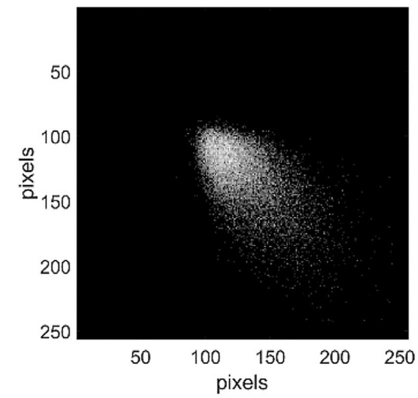

a) High activity THSP

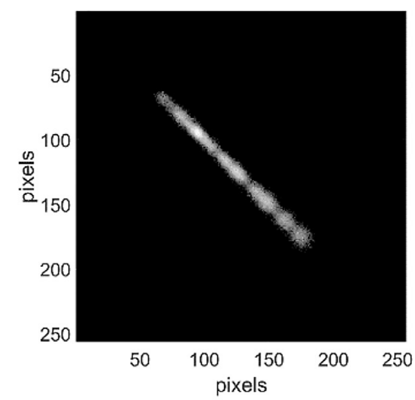

b) Low activity THSP

Fig. 6. Gray-level co-occurrence matrices.

4. Co-occurrence matrix

The 2D-THSP is then evaluated by using the Gray-Level Co-occurrence Matrix (GLCM), this matrix provides a distribution of co-occurring gray-level values given a position operator. In our case, as our interest is to evaluate temporal changes, these matrix is populated by calculating how often a pixel with a given gray-level value i occurs in the horizontal direction of an adjacent pixel with particular value j [13].

The principal diagonal from the GLCM is populated when there are no changes in the gray-level values in the horizontal direction. This implies that homogenous gray-level regions in the 2D-THSP will populate the region near this diagonal and further regions will be populated by high contrast change occurrences. As the activity in the 2D-THSP induce contrast changes, high activity the 2D-THSP will have disperse distributions in the GLCM and low activity will be centered in the principal diagonal as depicted in Fig. 6(a) and (b) respectively.

The spread from the values around the principal diagonal were calculated as the sum of the matrix location value times the horizontal distance from this value to the principal diagonal, this is known as contrast in the Haralick's texture descriptors, and is defined as a second-order moment called the inertia moment of the matrix along its principal di-

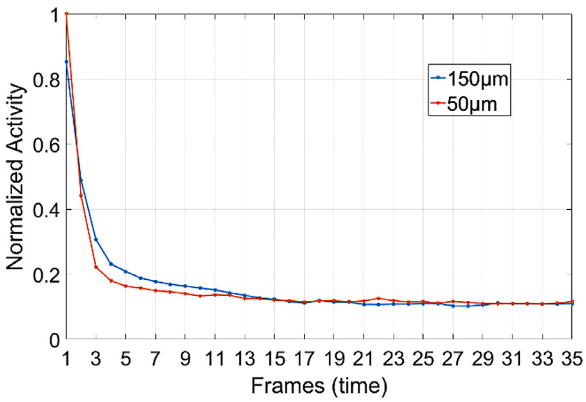

Fig. 7. Normalized activity calculated for 35 frames. In blue the activity changes for the right region (150 µm) and in red the left region (50 µm). (For interpretation of the references to color in this figure legend, the reader is referred to the web version of this article).

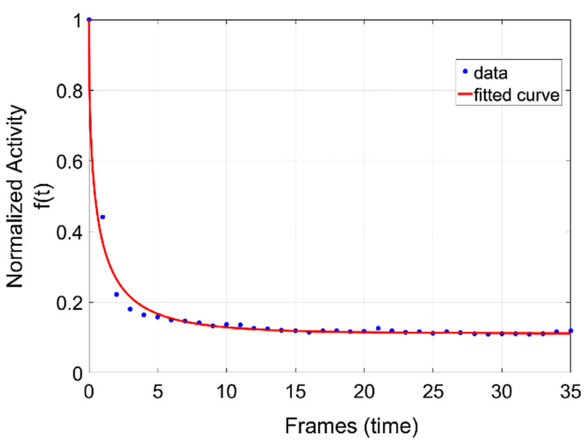

Fig. 8. Exponential squared-root decay fitted curve for the 50 µm coating level.

agonal:

$$IM = \sum_i \sum_j M_{ij}(i-j)^2 \tag{1}$$

where M_{ij} is the number of pixels with intensity i immediately followed by pixels with intensity j.

In order to calculate the normalized activity during the paint-coating drying process, the inertia moments from all the windows are then normalized by dividing their value by the highest activity value during the entire drying process.

5. Activity clusters

Activity evaluation on each window provides information about the local activity from the drying of the coating surface. This information makes feasible the recognition of regions in the activity images based on how active these regions are. In particular, we want to distinguish between: High, medium-high, medium, medium-low and low activity regions.

In order to group the windows' activity, we used a clustering algorithm based on the values normalized over all the samples. This shows how the five activity regions change over time without taking into account the spatial distribution from windows. In particular, we used K-means clustering, an unsupervised hard clustering algorithm that classifies a data collection into multiple classes [14]. The objective of the algorithm is to group a set of $\mathbf{x}_j,\ j = 1 \dots n$ vectors into $G_i,\ i = 1 \dots c$ different groups, by finding a cluster center such that a cost-function

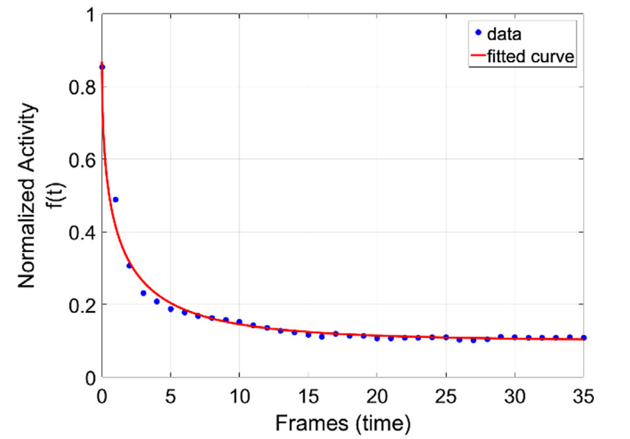

Fig. 9. Exponential squared-root decay curve fitting for the 150 µm coating level.

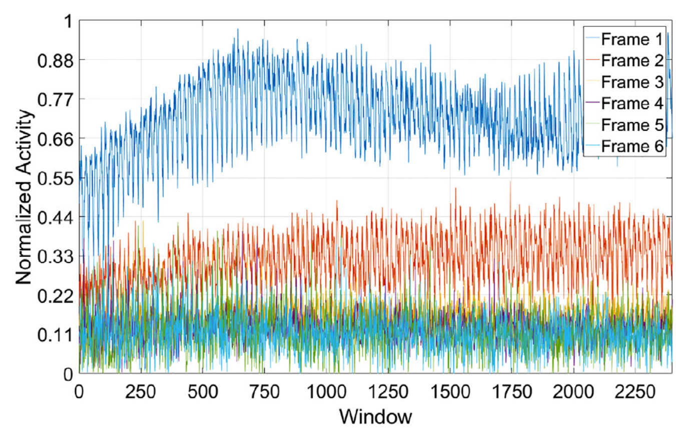

Fig. 10. Activity per window for the 50 µm coating layer.

defined by the distance measured from data to the cluster center is optimized. Using general definition of distance, the cost-function can be defined as

$$J = \sum_{i=1}^{c} J_i = \sum_{i=1}^{c} \left(\sum_{k, x_k \in G_i} d\left(x_k - c_i\right) \right) \tag{2}$$

To defined the membership of a vector to a particular cluster a membership matrix defined as:

$$u_{ij} = \begin{cases} 1 \ if \ d\left(x_j - c_i\right) \le d\left(x_j - c_k\right), \ \forall i \ne k \\ 0 \ otherwise \end{cases} \tag{3}$$

is employed, the vector $\mathbf{x}_j$ belongs to group c_i if this is the closest centre amongst the others. In this case element u_{ij} is 1 when data point x_j belongs to group i and 0 otherwise. This matrix has the following properties

$$\sum_{i=1}^{c} u_{ij} = 1,\ \forall j = 1 \dots n$$
$$\sum_{i=1}^{c} \sum_{j=1}^{n} u_{ij} = n \tag{4}$$

If u_{ij} is fixed, the optimal center c_i that minimizes (2) will be:

$$c_i = \frac{1}{|G_i|} \sum_{k, x_k \in G_i} x_k,\ |G_i| = \sum_{j=1}^{n} u_{ij} \tag{5}$$

6. Results and discussion

By using the experimental conditions described in Section 3, the paint-coating process was studied. First in Section 6.1 the speckle pat-

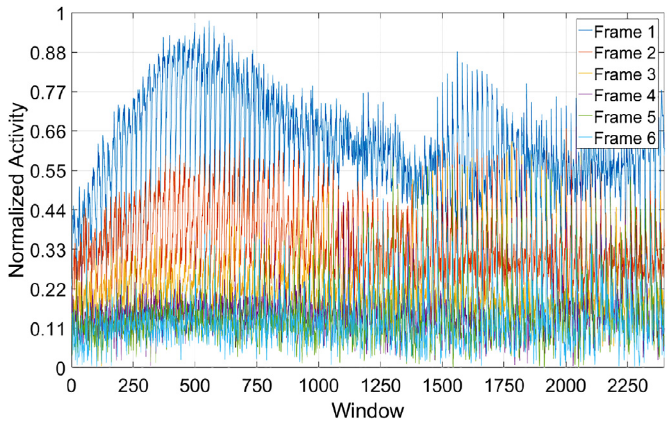

Fig. 11. Activity per window for the 150 µm coating layer.

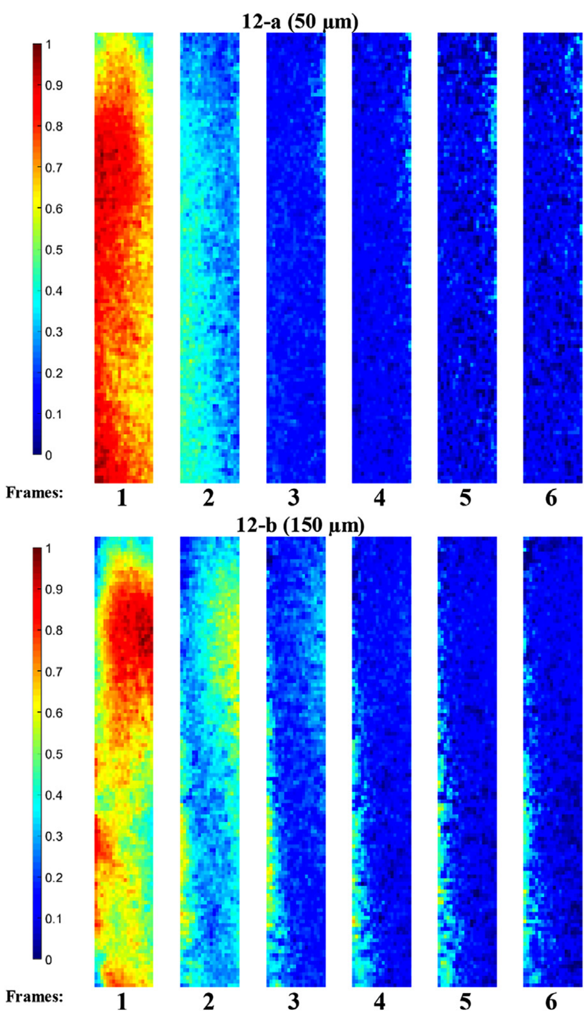

Fig. 12. Local activities per frame for 50 µm and 150 µm. Color-map corresponds with the window activity normalized for 50 and 150 µm together. (For interpretation of the references to color in this figure legend, the reader is referred to the web version of this article).

terns were evaluated by following the conventional THSP proposed by Amalvy et al. in [8]. In Section 6.2 the same dynamic speckle patterns are then processed using the new 2-dimensional temporal history speckle pattern (2D-THSP) in order to evaluate the local drying process. Finally, in Section 6.3, the proposed technique is compared with the gravimetric measurements.

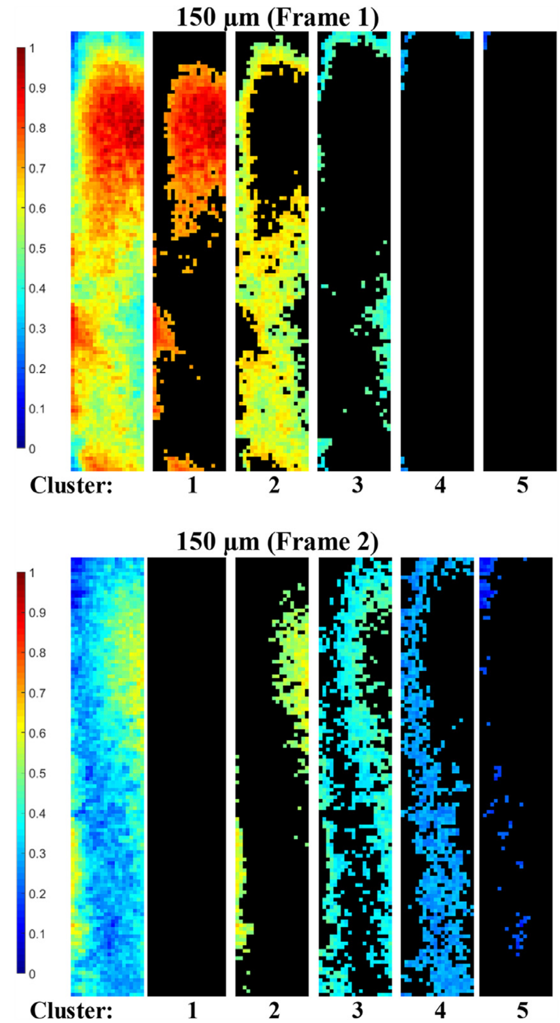

Fig. 13. Activity clusters for Frames 1 and 2 of the 150 µm layer.

6.1. Temporal history speckle pattern (THSP)

The paint-coating was recorded for 525 min corresponding to 35 frames. As it was stated before each frame is the result of the processing from 1000 images taken every 0.9 s, both coatings reach steady state by frame 16 implying that both paint layers are dry. The obtained experimental data processed by using the THSP method is presented in Fig. 7. It should be noted that the activity from the region with 150 µm (blue) is higher than the activity from the 50 µm layer (red) which present a slightly higher drying coefficient. Albeit some differences between both curves, this changes are not easily addressed.

This data is then fitted following the exponential squared-root decay model [15], to calculate drying model parameters. Exponential squared-root decay fitted curve for the 50 µm and 150 µm coating layers are presented in Figs. 8 and 9 respectively.

The corresponding equation for the 50 µm layer fitted data is:

$$f(t) = 0.89e^{-1.243\sqrt{t}} + 0.11 \tag{6}$$

The curve fitting model in this case (150 µm) is:

$$f(t) = 0.767e^{-0.8956\sqrt{t}} + 0.1 \tag{7}$$

6.2. 2D temporal history speckle pattern (2D-THSP)

When the 2D-THSP windows are created for each of the frames the activity differences between windows become apparent. The dynamic

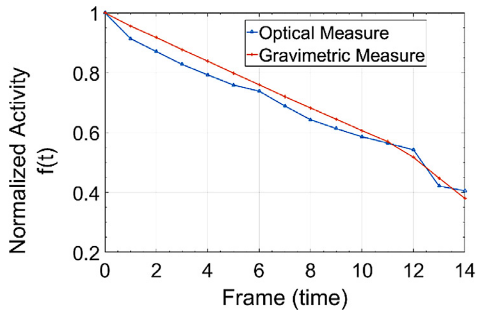

Fig. 14. Comparison between the optical (blue) and the gravimetric measurement (red). (For interpretation of the references to color in this figure legend, the reader is referred to the web version of this article).

speckle patterns from frames were divided in windows starting from the upper left corner, going first through the rows and then the columns. These 2D-THSP windows were obtained for both right and left part of the dynamic speckle patterns corresponding to 50 µm and 150 µm respectively. As each window consist in the activity matrix for a 5 × 5 sub-matrix from the dynamic speckle images, since our image size in the experiments was 600 × 100 (60,000 pixels) and a window size of 5 × 5 (25 pixels) represents only 0.041% of the total image hence the analysis is considered local. In our case the frames are constituted by 20 × 120 windows (each window containing a 25 × 1000 pixels activity matrix), giving 2400 windows in total. In Figs. 10 and 11 the normalized activity calculated per window is presented, it should be noted that due to the window selection the first windows represented in the graphic correspond to the upper edge from speckle pattern and growing in the direction of the central region, the average frame normalized activity decay following the exponential squared-root model.

It is apparent that the activity changes between windows corresponding to the frame 1 of the 50 µm coating layer is higher than the 150 µm coating layer (see Figs. 10 and 11). These results confirm the necessity to evaluate the local activity and their contribution to understanding the process progress.

By following our proposal, the edge effects can be considered and analyzed, the presented results confirm the changes in the thickness of the paint-coating films at the periphery of sample glass plate. This effect can be inferred by observing the local speckle time evolution. It is expected that the paint layer thickness variations, throughout the sample, influence the gravimetric data. Previous results as presented in [8–10] only considered the optical data collected in the central zone of the sample.

Once the normalized activity is evaluated on each window, the frames can be recomposed providing a local activity map from the dynamic speckle patterns and consequently of the local activity of the paint-coating drying process. Fig. 12 represents the local activity from the first 6 frames chronologically arranged, these frames represent a total of 75 min, meaning that each frame is spaced 15 min. In this particular experiment, each frame represents a temporal state, and is obtained by processing the set of 1,000 images taken every 0.9 seconds. Fig. 12(a) represents the results for 50 µm and Fig. 12(b) for 150 µm layers. Both Figures include the respective color maps indicating the activity, as expected the 50 µm layer portrays higher activity on frame 1 and higher decay rate. The 150 µm layer portrays less activity on frame one but remains active for more time.

In order to provide an easy way to address the state of the paint-coating drying process we separated the activity in 5 regions: High, medium-high, medium, medium-low and low activity. The normalized activity was clustered using K-means algorithm using Euclidean distance metrics for 5 clusters, this provides a convenient classification as presented in Fig. 13 for the drying process in possible applications of the proposed technique.

6.3. Technique validation

The optical measurements were compared with the gravimetric measurements, a gold standard in the paint industry. Paint thickness and environmental conditions were kept constant. A single coating layer with an average thickness of 50 µm was applied over the glass substrate. A sequence of 8-bits gray scale images (512 × 512 pixels) dynamic speckle patterns were registered using a PULNIX TM-6CN CCD monochrome camera connected to a PC. 350 successive digitalized images were recorded every 5 min during 120 min, this particular experiment has 14 frames. Activity evaluation on each window is determined following the proposed procedure.

When comparing the gravimetric measurement with the optical measurement the error ranges from 0.84% to 6.67% with an average of 4.34%. The error ranges are percentages, and as the values tend to zero the percentage seems higher despite a reduction in the absolute error values. The comparison between the average normalized window activity from frames and the gravimetric measurement is presented in Fig. 14, the blue line corresponds with the optical measurements and the red line to the gravimetric measurement. In Fig. 15 shows the local activity from this experiment for each of the frames with the corresponding color map for the normalized activity when a 510 rows × 100 columns region from the center of the speckle patterns were selected.

7. Conclusions

We have presented a technique based on dynamic speckle patterns, useful for the local evaluation of paint-coating drying process.

In real experiments, the paint layers have different thickness in different regions as the coating application is not perfectly homogeneous. The speckle patterns from our experiments are recorded using an image formation system. This implies that the retrieved information from the detector preserves the local information from the paint sample. Therefore, the use of a vertical line as in the conventional TSPI based on image

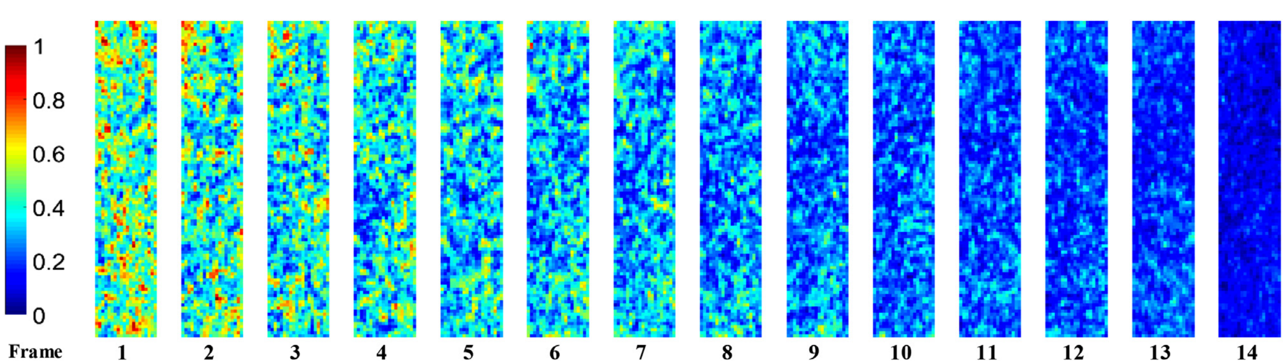

Fig. 15. Local activity for the 14 frames of the validation experiment.

formation system is not as convenient because different regions involve different thickness in the line used for assessment. With our proposal, we have extended the paint coating drying analysis to a local regime, the defined window matrix allows us to address a localized region with approximately the same thickness.

From the dynamic speckle patterns, a new 2-dimensional temporal history of speckle was generated by the selection and processing of 5×5 windows, those windows allow for the local activity assessment. The activity obtained from each window was then clustered in order to obtain five different classes: High, medium-high, medium, medium-low and low activity. These classes provide a convenient classification of the drying process, looking forward to the constitution of a future framework for industrial applications. With this work, we have extended the application from the techniques for paint-coating drying evaluation based on dynamic speckle patterns to address the local activity from coatings. The experimental data in this work was compared with the previous proposals, including in its formulation the mathematical model for the exponential squared-root decay fitting. An average error of 4.34% was obtained when comparing the optical measurements using the proposed technique with the gravimetric measurements, gold standard in the industry. We foresee that the proposed technique can be used on industrial applications for drying time addressing, quality control, among others.

Acknowledgments

This research was performed under the grants: CONICET Nos. 0849/16 and 0549/12 (Argentina) and Facultad Ingenería, Universidad Nacional de La Plata Nos. 11/I215 and 11/ I192 (Argentina).

References

[1] Sirohi RS, editor. Speckle metrology. Marcel Dekker; 1993.
[2] Rabal HJ, Braga RA, editors. Dynamic laser speckle and applications. CRC Press; 2008.
[3] Braga RA, Dal Fabbro IM, Borem FM, Rabelo G, Arizaga R, Rabal HJ, Trivi M. Assessment of seed viability by laser speckle techniques. Biosyst Eng 2003;86(3):287–94.
[4] Pajuelo M, Baldwin G, Rabal H, Cap N, Arizaga R, Trivi M. Bio-speckle assessment of bruising in fruits. Opt Lasers Eng 2003;40(1):13–24.
[5] Jr Braga, A R, Rabelo GF, Granato LR, Santos EF, Machado JC, Arizaga R, Trivi M. Detection of fungi in beans by the laser biospeckle technique. Biosyst Eng 2005;91(4):465–9.
[6] Murialdo SE, Sendra GH, Passoni LI, Arizaga R, Gonzalez JF, Rabal H, Trivi M. Analysis of bacterial chemotactic response using dynamic laser speckle. J Biomed Opt 2009;14(6) 064015-064015.
[7] Wachowiak MP, Smolikova R, Tourassi GD, Elmaghraby AS. General ultrasound speckle models in determining scatterer density. Proc. SPIE 2002;4687:285–95.
[8] Amalvy JI, Lasquibar CA, Arizaga R, Rabal H, Trivi M. Application of dynamic speckle interferometry to the drying of coatings. Prog Org Coat 2001;42(1):89–99.
[9] Mavilio A, Fernández M, Trivi M, Rabal H, Arizaga R. Characterization of a paint drying process through granulometric analysis of speckle dynamic patterns. Signal Process May 2010;90(5):1623–30.
[10] Blotta E, Ballarín V, Brun M, Rabal H. Evaluation of speckle-interferometry descriptors to measuring drying-of-coatings. Signal Process 2011;91(10):2395–403.
[11] Passoni I, Dai Pra A, Rabal H, Trivi M, Arizaga R. Dynamic speckle processing using wavelets based entropy. Opt Commun 2005;246(1-3):219–28.
[12] Limia MF, Nunez AM, Rabal H, Trivi M. Wavelet transform analysis of dynamic speckle patterns texture. Appl Opt 2002;41(32):6745–50.
[13] Haralick RM, Shanmugam K. Textural features for image classification. IEEE Trans Syst, Man, Cybern 1973(6):610–21.
[14] Tan PN. Introduction to data mining. India: Pearson Education; 2006. p. 496–515.
[15] Howison SD, Moriarty JA, Ockendon JR, Terrill EL, Wilson SK. A mathematical model for drying paint layers. J Eng Math 1997;32(4):377–94.